Author accepted copy

Accepted for publication 15/02/2022

Challenges and perspectives for integral bridges in the UK: from design practice to fieldwork through small-scale laboratory experiments

Sha Luo
Research Associate, University of Birmingham, Birmingham, UK
Email: s.luo@bham.ac.uk
ORCID: 0000-0002-1257-4998

Flavia De Luca
Senior Lecturer, University of Bristol, Bristol, UK
Email: flavia.deluca@bristol.ac.uk (Corresponding Author)
ORCID: 0000-0003-2387-8580

Raffaele De Risi
Lecturer, University of Bristol, Bristol, UK
Email: raffaeele.derisi@bristol.ac.uk
ORCID: 0000-0002-5496-9656

Louis Le Pen
Senior Research Fellow, University of Southampton, Southampton, UK
Email: louis.lepen@soton.ac.uk
ORCID: 0000-0002-4362-3895

Geoff Watson
Research Fellow, University of Southampton, Southampton, UK
Email: g.watson@soton.ac.uk
ORCID: 0000-0003-3074-5196

David Milne
Research Fellow, University of Southampton, Southampton, UK
Email: d.milne@soton.ac.uk
ORCID: 0000-0001-6702-3918

David Chapman
Professor, University of Birmingham, Birmingham, UK
Email: d.n.chapman@bham.ac.uk
ORCID:

Anastasios Sextos

Professor, University of Bristol, Bristol, UK
Email: a.sextos@bristol.ac.uk
ORCID: 0000-0002-2616-9395

Nigel Cassidy
Professor, University of Birmingham, Birmingham, UK
Email: n.j.cassidy@bham.ac.uk
ORCID: 0000-0002-1492-5413

Ian Jefferson
Professor, University of Birmingham, Birmingham, UK
Email: i.jefferson@bham.ac.uk
ORCID: 0000-0001-6437-101X

Nicole Metje
Professor, University of Birmingham, Birmingham, UK
Email: n.metje@bham.ac.uk
ORCID: 0000-0002-6741-8183

Joel Smethurst
Associate Professor, University of Southampton, Southampton, UK
Email: J.A.SMETHURST@soton.ac.uk
ORCID: 0000-0001-8175-985X

David Richards
Professor, University of Southampton, Southampton, UK
Email: djr@soton.ac.uk
ORCID: 0000-0002-3819-7297

George Mylonakis
Professor, University of Bristol, Bristol, UK
Email: g.mylonakis@bristol.ac.uk
ORCID: 0000-0002-8455-8946

Colin Taylor
Emeritus Professor, University of Bristol, Bristol, UK
Email: colin.taylor@bristol.ac.uk
ORCID: 0000-0002-2201-8231

William Powrie
Professor, University of Southampton, Southampton, UK
Email: w.powrie@soton.ac.uk
ORCID: 0000-0002-2271-0826

Christopher D.F. Rogers
Professor, University of Birmingham, Birmingham, UK
Email: c.d.f.rogers@bham.ac.uk
ORCID: 0000-0002-1693-1999

Word count in the main text: ~7000 words

Challenges and perspectives for integral bridges in the UK: from design practice to fieldwork through small-scale laboratory experiments

Sha Luo[1], Flavia De Luca[2], Raffaele De Risi[2], Louis Le Pen[3], Geoff Watson[3], David Milne[3], David Chapman[1], Anastasios Sextos[2], Nigel Cassidy[1], Ian Jefferson[1], Nicole Metje[1], Joel Smethurst[3], David Richards[3], George Mylonakis[2], Colin Taylor[2], William Powrie[3], Christopher D.F. Rogers[1]*

[1] School of Engineering, University of Birmingham, Edgbaston, B15 2TT (UK)

[2] School of Civil, Aerospace and Mechanical Engineering, University of Bristol, Queens Building, BS8 1TR (UK)

[3] Infrastructure Research Group, Faculty of Engineering and the Environment, University of Southampton, Southampton, UK

ABSTRACT

This study focuses on the investigation of the factors that have limited, so far, the development of a consistent design and assessment approach for integral bridges (IBs). This paper presents a review of previous research and current design practices for IBs, followed by a review of monitoring studies in the laboratory and in the field. As part of the UKCRIC PLEXUS experimental campaign, a small-scale 1g physical experiment is described. The test aimed to simulate the soil-structure interaction arising from seasonal expansion and contraction of the bridge deck and assess the performance of different monitoring techniques. Pressure cells were used to measure the lateral stresses behind the abutment wall, Particle Image Velocimetry was employed to monitor the soil behaviour behind the abutment and Linear Variable Differential Transformers were used to monitor the backfill surface movements. By combining the data from these instruments, a preliminary assessment of the soil-structure interaction behaviour of the idealised integral abutment under seasonal thermal loading has been obtained. These monitoring methods and the associated understanding of IBs' behaviour gained from the tests provide definitive evidence for the development of monitoring systems for larger-scale physical tests and field monitoring systems for IBs.

Keywords

Bridges; thermal effects; laboratory tests; earth pressure; settlement; monitoring; soil/structure interaction

*Corresponding author: flavia.deluca@bristol.ac.uk

List of notation

K lateral earth pressure coefficient

K_0 horizontal earth compression coefficient, at rest

K_a horizontal earth compression coefficient, active

K_p horizontal earth compression coefficient, passive

d displacement at the top of the bridge abutment due to thermal loading

α coefficient of thermal expansion of the deck (of the order of 10^{-5} for concrete decks)

L_X expansion length measured from the end of the bridge to the position on the deck that remains stationary when the bridge expands

$T_{e;max}$ characteristic maximum uniform temperature for a 50-year return period in the UK

$T_{e;min}$ characteristic minimum uniform temperature for a 50-year return period in the UK

$\emptyset$ slope of the earth pressure

H height of the abutment

d'_d wall deflection at depth $H/2$ below ground level

K_d^* design value of the earth pressure coefficient for expansion

C dimensionless coefficient used in the calculation of K_d^*

$K_{p;t}$ coefficient of passive earth pressure used in the calculation of K_d^*

ϕ' effective friction angle

c'_{peak} peak effective cohesion

φ'_{peak} peak effective friction angle

e_{min} minimum void ratio

e_{max} maximum void ratio

ε soil volumetric strain

1. Introduction

A large investment is continually made in infrastructure globally. For example, the UK infrastructure pipeline has committed £12.6bn for roads and £46.2bn for rail (National Infrastructure Delivery Plan 2016-2021). Internationally, the global pipeline is estimated to be as high as US$97 trillion (Global Infrastructure Hub, 2020). In transportation networks, bridges represent a particularly vulnerable element to which the largest investment is linked (e.g., Rasulo et al. 2004; Nuti et al. 2009; Thoft-Christensen 2012; NIST 2015). In traditional bridges, joints and bearings have emerged as the main source of bridge maintenance problems and costs (Wolde-Tinsae and Greimann, 1988; Greimann and Wolde-Tinsae, 1986) due to the cyclic displacements caused by thermal gradients, traffic and dynamic loads, while both corrosion of and access to bearings provide particular maintenance challenges. Thus, integral bridges (IBs) are becoming increasingly attractive because of reduced maintenance issues at the bridge deck–abutment interface compared with traditional bridge construction.

Integral bridges have received increasing attention by designers in the last few decades and are widely used in many countries for small-to-medium span highway bridges and overcrossings (Burke, 2009). They now constitute a significant part of the transportation infrastructure stock, with an estimated number in service of over 9,000 in the US alone (Paraschos and Amde 2011; White et al. 2010; Fiorentino et al 2021). Integral bridges are likewise becoming more widely used in the United Kingdom, Europe and Asia (Bloodworth, 2011), while their design varies according to practices and requirements outlined by regional transportation authorities. In the United States, each state highway department has its integral abutment programme and has established guidelines concerning their design and construction. The specification of the American Association of State Highway and Transportation Officials (AASHTO LRFD; AASHTO, 2012) is the most widely accepted integral bridge design guideline in the United States, providing performance criteria for IB design. Parallel design guidance is provided in the Canadian Foundation Engineering Manual (Canadian Geotechnical Society, 1978).

In the UK, PD 6694 (PD 6694-1: 2011) and the Highways Agency Design Manual for Roads and Bridges (BA42/96 2003) are currently the reference guides, with these documents referring to European standards (EN 1997-1, Eurocode 7) and CIRIA Report 760 on embedded retaining walls (Gaba et al., 2017) for relevant design parameters. Currently, span lengths of integral bridges are limited due to the lack of an adequate evidence base on which to predict their performance. There is consequent conservatism in design guidance (Dicleli et al. 2003; Baptiste et al. 2011, Zordan 2011a; Zordan 2011b; Mitoulis et al. 2016), which, in turn, reflects imperfect understanding of the behaviour of these structures under the imposed loads. In the UK, spans are limited to 60 m length and 30 degrees skew (BA42/96 2003, PD 6694 2011). Although design codes offer provision for the static design of integral bridges (BMVBS 2013; Gaba et al. 2017), the use of IBs is limited mainly by the lack of explicit design guidelines coherent across different countries.

The rationale for the limitations in design codes lies mainly in the uncertainty related to the soil-structure interaction between the backfill and the abutment walls when integral bridge decks expand due to seasonal thermal loads under ambient conditions (Gorini and Callisto, 2017; 2019; Huffman et al., 2015). When the bridge expands, substantial force is exerted on the abutment by the soil reaction, and this can significantly impact the integrity of the structure. Such inherently nonlinear soil action is dependent on the magnitude and distribution (with height) of the wall displacement, which encompasses both translational and rotational displacements depending on the boundary conditions. In the longer term, as seasons of cyclic expansion and contraction of the bridge decks occur, there can be a build-up of significant lateral earth pressure behind the abutments (Figure 1a). This asymmetric cyclic stress-strain behaviour is known as *ratcheting* (Horvath, 2004; Cui and Mitoulis, 2015; England et al. 2000). However, soil conditions can vary from relatively loose to dense states with different compaction levels; consequently, the pressure that builds-up behind the abutment could significantly increase with time – by a factor of four or more. Accordingly, axial forces on the bridge deck may increase as well, by a factor of around two (part of the pressure being absorbed by the abutment foundation), while bending moments in the composite deck may increase by somewhat less than the axial forces, depending on soil stiffness and boundary conditions (Fennema et al., 2005; Shamsabadi et al., 2007; Clayton et al., 2006; Mahjoubi and Maleki, 2018). The thermal loading also causes ground settlement adjacent to abutments (which may be under approach slabs, if present), with gaps often observed at the surface between the abutment and backfill (Figure 1b). Moreover, subsidence behind the abutment wall can cause structural problems in approach slabs if the bending loads due to traffic are significant (Muttoni et al., 2013).

A number of mitigation measures are available to reduce the excessive lateral pressures on the abutment walls. These include limiting bridge length, skew and the vertical penetration of abutments into embankments; using selected granular backfill (Al-Ani et al., 2018); providing approach slabs to prevent vehicular compaction of the backfill (Muttoni et al., 2013); using embankment benches to shorten wing walls; and using suspended turn back wing walls (Paraschos, 2016).

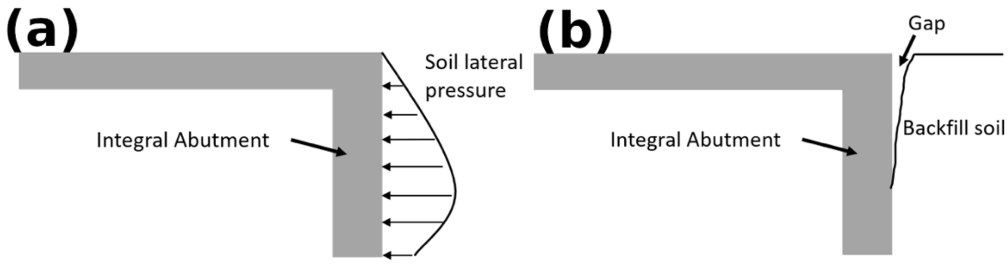

Figure 1. (a) build-up of lateral earth pressures behind the abutment under thermal loading, (b) gapping between abutment wall and backfill under cyclic thermal loading.

In addition, semi-integral abutment designs (Figure 2) are used to remove passive pressures under bridge seats. In such designs, the end screen wall and deck beams are integral with each other, but the end screen wall does not provide support to the deck beams. Instead, a structure with bearings, which can accommodate horizontal displacement, is provided as support to the deck beams.

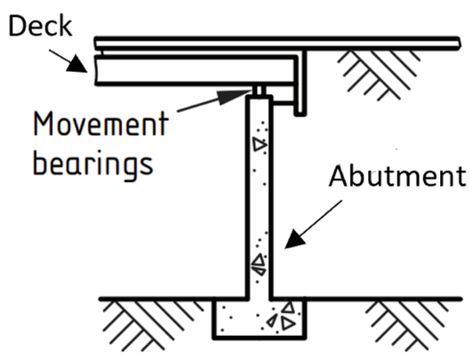

Figure 2. Semi-integral abutment design (from PD6694, 2011)

Compressible inclusions between the abutments and the backfill, such as EPS Geofoam, have also been proposed to mitigate the build-up of earth pressures and uncouple the response of the bridge from that of the backfill (Horvath 2000, 2005, Mylonakis et al. 2007a, Mitoulis et al. 2016, Fiorentino et al. 2021). However, extra design and construction work should be allowed for at the design stage. Compressible inclusions between the abutment and the backfill allow dissipation of the lateral earth pressures and the control of displacements in the backfill in performance-based design (Karpurapu and Bathurst 1992, Abdel Salam and Azzam 2016).

It has also been observed that even if the superstructure responds linearly elastically under thermal loads (which is anticipated in IBs), local nonlinear material behaviour of the backfill could result in triggering a nonlinear response in the entire soil-bridge system (McCallen et al. 1994). Recurrent cyclic traffic loads during integral bridge operation (assuming there is no bridging slab) further compacts the backfill, and may also contribute to increases in lateral earth pressures. These effects can be replicated through mechanistic models that have been proposed for the numerical modelling of soil-structure interaction effects on integral bridge abutments (Zhang and Makris 2002, Kotsoglou and Pantazopoulou 2007, 2009; Kappos and Sextos 2009).

A field study of an integral bridge equipped with an elastic inclusion (i.e., a layer of elastic material between the abutment and the retained soil) showed significantly reduced lateral earth pressures and tolerable settlements of the approach fill (Hoppe, 2005). This isolated system exhibited a mirrored behaviour, with increasing pressure effects occurring at each consecutive thermal cycle, while the backfill soil displacements showed a settling effect with a decreasing magnitude with increasing number of cycles. An important finding was that both the developed pressures and the associated displacements were smaller than those in the conventional system: the peak pressures were seven times smaller and the settlement around four times smaller. Due to the lower absolute pressures and an approximately linear pressure distribution behind the abutment, the overall bending moments induced on the abutment walls were also greatly reduced. This approach may, therefore, lead a more sustainable solution to span longer distances (Caristo et al., 2018). However, without explicit adoption in codes, elastic inclusions are unlikely to achieve widespread use and there remain maintenance implications that can make this solution less appealing.

Reducing or removing uncertainties/barriers and improving the functionality of IBs, throughout their design, construction, operation and maintenance phases, provide a means of reducing infrastructure costs and increasing their value. This can be achieved by better diagnosis (i.e., developing knowhow on the problem to reduce epistemic uncertainty) and feeding research findings from laboratory experiments, modelling and field-monitoring campaigns into national and international design code development (Dhar and Dasgupta 2019). In support of this and similar goals, the UK Collaboratorium for Research on Infrastructure and Cities

(UKCRIC; www.ukcric.com), has recently created a suite of world-leading laboratory facilities combining multi-disciplinary research teams with systems thinking and practice approaches to enhance the value of, and de-risk investments in, infrastructure and urban systems interventions.

The UKCRIC–PLEXUS (Priming Laboratory EXperiments on infrastructure and Urban Systems) programme included a project that combined three of the new national facilities and a variety of research approaches to establish a comprehensive picture of the soil-structure interaction behaviour of IB abutments under lateral loading. This included a small-scale experimental campaign to complement the evidence base available in the literature, which is reported herein following a brief review of current international design practices (Section 2), an introduction to previous field monitoring techniques (Section 3) and a review of previous research on IBs (Section 4). The results from the experimental campaign (Section 5) are then presented and discussed in relation Sections 1-4, along with conclusions and plans for large-scale experimental tests (Section 6).

2. Current design practice

The design of IBs varies according to practices and requirements stipulated by local transportation agencies, a brief summary is presented in Table 1. The US (AASHTO, 2012), Canadian (Canadian Geotechnical Society, 1978) and UK (PD 6694-1: 2011; BA42/96 2003) guidance are perhaps the most authoritative.

For abutment design, the earth pressure distribution behind the abutment is determined using a depth-dependent lateral earth pressure coefficient, K (Mei et al., 2017; Vahedifard, 2015), defined as the ratio of effective lateral (horizontal) effective stress to the effective vertical stress at a specific depth. The value of K depends on many parameters, notably the nature of soil (coarse grained vs fine grained), its density and its loading history (over-consolidation ratio). There are three categories of horizontal earth pressure coefficient: at rest (K_0) corresponding to zero horizontal wall movement and zero normal horizontal soil strain, active (K_a) representing a theoretical minimum value requiring sufficient outward wall displacement (i.e., away from the backfill), and passive (K_p) representing a theoretical maximum value requiring sufficient inward wall displacement (towards the backfill). There are several, theoretical and empirical, theories for establishing the lateral earth pressure coefficient. Coulomb (1773) first proposed a heuristic limit analysis framework (known today as the Limit Equilibrium method) associated with shear failure of a soil wedge within the backfill, using an optimisation procedure to identify stationary values among an infinite set of candidate lateral thrusts. Mayniel in 1808 extended Coulomb's equations to include wall friction, and Muller-Breslau in 1906 further generalised Mayniel's equations to incorporate an inclined backfill and wall. Coulomb's solution provides the most useful tool for establishing earth thrusts by hand calculations, yet the method works solely with forces (not stresses) and thus cannot establish the point of application (elevation) of the overall soil thrust. Subsequently, Rankine's (1857) theory, based on limit stresses to predict active and passive pressure coefficients, produced exact stresses (hence predicting the point of application of soil thrust). However, its applicability is limited – notably to vertical walls having roughness equal to the inclination of the backfill under plane strain conditions – while the kinematics of the problem (i.e., soil and wall displacements) and the compatibility of deformations are essentially ignored. More advanced stress solutions encompassing inclined backfill and wall are available in Mylonakis et al. (2007b).

Importantly, the use of full passive pressures without regard to displacements and compatibility of deformations is not conservative as it invariably suppresses the flexural effects of dead and live loads on the bridge girders. Modified coefficients based on Rankine's solution have been proposed (Kloukinas et al 2015; Hanna and Diab, 2016; Pain et al., 2017; Rajesh and Choudhury, 2017). For relatively short single-span IBs, the passive earth pressure coefficients were reduced by multiplying the relevant Rankine coefficients with modification factors. The displacement at the top of the bridge abutment due to thermal loading, d, is calculated using Equation 1 (PD6694, 2011):

$$d = \alpha \, L_X \, (T_{e;max} - T_{e;min}) \qquad (1)$$

where:

α is coefficient of thermal expansion of the deck (of the order of 10^{-5} for concrete decks);

L_X is expansion length measured from the end of the bridge to the position on the deck that remains stationary when the bridge expands;

$T_{e;max}$ and $T_{e;min}$ are the characteristic maximum and minimum uniform bridge temperature components for a 50-year return period in the UK (National Annex to BS EN 1991-1-5, 2003), respectively.

The specified dimensionless displacement (“drift”, which is the horizontal movement applied on the top of the abutment wall from span over the abutment wall height) for full passive pressure development is equal to approximately 4 x 10^{-2} for loose sand and equal to 1 x 10^{-2} for dense sand (Clough and Duncan, 1991). Widely used curves to determine the lateral soil pressure for loose, medium and dense granular materials (Figure 3) are presented in NCHRP Report 343 (NCHRP, 1991) and NAVFAC (1982), while design curves are provided in the Canadian Foundation Engineering Manual (Canadian Geotechnical Society, 1978) and by the US Section of the Navy (Cole and Rollins, 2006).

NCHRP (1991) and NAVFAC (1982) recommend applying limit equilibrium solutions based on log spiral failure mechanisms for standard backfill configurations, since Coulomb’s failure wedge methodology is notoriously non-conservative for determining passive pressures (Xu et al., 2018; Keykhosropour, and Lemnitzer, 2019). AASHTO (2012) determines horizontal soil pressures on bridge abutments according to Rankine’s active soil pressures, based on variations in the earth pressure coefficient as a function of structural displacement from experimental data and finite element analyses, leading to a practically linear relationship as shown in Equation 2 (Bal et al., 2018; Capilleri et al., 2019):

$$K = K_0 + \emptyset\, d \leq K_p \qquad (2)$$

where d is the displacement of the IB towards the backfill, and $\emptyset$ is the slope of the earth pressure variation with horizontal displacement (which varies with the backfill type).

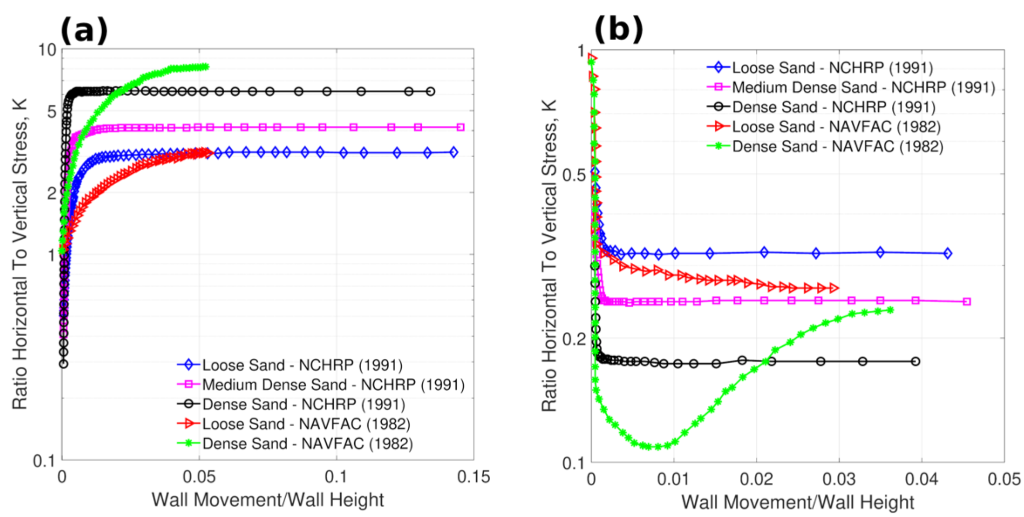

Figure 3. Relationship between wall displacement and earth pressure in sand (a) wall moving towards the backfill (passive like) (b) wall moving away from the backfill (active like) according to NCHRP (1991) and NAVFAC (1982).

There is reasonable agreement between the predicted average passive earth pressure of standard compacted gravel backfill with the results from full-scale wall tests performed at the University of Massachusetts (Bonczar et al., 2005). According to the tests, the pressure coefficient K (Massachusetts Bridge Manual, 1999) can be estimated using the following empirical equation:

$$K = 0.43 + 5.7\left[1 - e^{-190\left(\frac{d}{H}\right)}\right] \quad (3)$$

where d is the displacement of the IB towards the backfill soil, and H is the height of the abutment. The first term in Equation 3 (0.43) can be interpreted as a K_o coefficient, while the multiplier on the second term (5.7) can be interpreted as the difference between passive and at rest pressures (K_p – K_o), being zero for zero displacement and maximum (5.7) for infinite displacement. To achieve a pressure equal to 99% of active requires a dimensionless displacement ("drift") of approximately 2.4%. These values correspond to the case of a rough wall and a medium-dense granular backfill.

From experiments investigating the cyclic stresses in backfill soil on a concrete wall with a pinned connection to a strip footing (Firoozi et al., 2016; Yazdandoust et al., 2019), and according to PD 6694 (2011) for full height abutments on spread footings, which accommodate thermal movements by rotation or flexure, the earth pressure on the retained face for an integral abutment wall is dependent on: (1) the thermal movement range (based on a 50-year return period), (2) the direction of movement (expansion or contraction), and (3) the magnitude of expansion or contraction for the combination of actions for the design situation under consideration (Figure 4). The design value of the earth pressure coefficient for expansion K_d^* can be estimated from Equation 4, but should not be taken as greater than $K_{p;t}$:

$$K_d^* = K_0 + \left(\frac{C d_d'}{H}\right) K_{p;t} \quad (4)$$

where K_0 is the coefficient of earth pressure at rest; H is the vertical distance from ground level to the level at which the abutment is assumed to rotate; d_d' is the wall deflection at depth $H/2$ below ground level; C is a dimensionless coefficient equal to 20 for foundations on loose soils with Young's modulus $E \leq 100$ MPa, and 66 for foundations on rock or soils with $E \geq 1000$ MPa, and which may be determined by linear interpolation for values of between 100 MPa and 1000 MPa; $K_{p;t}$ is the coefficient of passive earth pressure used in the calculation of K_d^*.

Design guidance for IBs is developing worldwide with a particular focus on the effect of thermal loading. However, there are still unanswered questions related to longer-term effects due to cyclic loading, notably does the earth pressure distribution change after many years of thermal cycling loading, and should the cycling loading history be considered in the estimation of the lateral pressure distribution behind the abutment?

It is evident, therefore, that the design methods provided in guidelines are characterised by significant uncertainty on the degree of conservatism embedded in the methods and lack consistency between countries. This emphasises the need for further investigation both under controlled condition in laboratories and via monitoring of IBs in the field, notably focussing on the abutment and associated backfill behaviour during a large number of repetitive cycles of displacement.

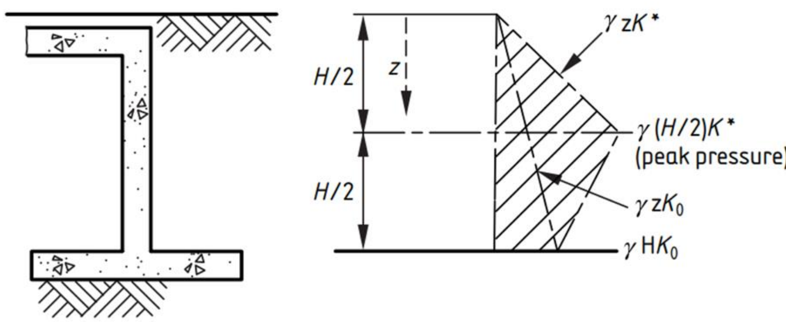

Figure 4. Earth pressure distributions for abutments that can accommodate thermal expansion by rotation and/or flexure (from PD6694, 2011), where K_0 is the coefficient of earth pressure at rest; H is the vertical distance from ground level to the level at which the abutment is assumed to rotate; γ is united soil weight; z is the soil depth; K^* is the design value of the earth pressure coefficient for expansion.

Table 1. Summary information of design guidance. (Note that limit equilibrium methods cannot predict distributions of passive pressures with depth. Accordingly, additional assumptions are needed to predict shear forces and bending moments at the two end of the wall).

Design guidance	**Region**	**Estimation of earth pressures**	**Limiting Design Criteria**
AASHTO LRFD, 2012	USA	The earth pressure coefficient variations are a function of structural displacement from experimental data and finite-element analyses, leading to a quasi-linear relationship	The limiting design criteria varies in different states. In 1980, American Federal Highway Association (FHWA) recommended: steel bridge - 90m; cast-in-place concrete bridge - 150m; post-tensioned bridges - 183m.
NCHRP, 1991		Limit equilibrium solutions based on log spiral failure mechanisms for standard backfill configurations (loose, medium and dense sand)	
NAVFAC, 1982		Limit equilibrium solutions based on log spiral failure mechanisms for standard backfill configurations (loose and dense sand)	
U.S. Department of Navy, 1982		Terzaghi's log spiral wedge theory to determine passive soil pressure coefficient	
Massachusetts Bridge Manual, 1999		Provided the equations (according to full-scale wall tests) to calculate the design earth pressure distribution behind the abutment of IABs	
Canadian Geotechnical Society, 1978	Canada	The soil pressure coefficients are based on the thermal movement of the model, vary with abutment rotation.	Different provinces have their own design guidance. For example, Alberta limited the span of IABs to 100m, with skew angle less than 20 degrees. Ontario limited the height of the abutment to 7m and length of wingwall to 6m.
PD6694,2011	UK	Limit equilibrium approach and SSI analysis	Span length - 60m; skew - 30 degree; the characteristic thermal movement of the end of the deck is less than or equal to 40 mm.

3. Field monitoring of IBs

Field monitoring data from in-service IBs is significant both to inform and improve future design guidance, and to refine experimental and numerical research. Many IBs globally are currently being monitored, see Table 2 for a general overview of significant monitoring studies. One of the monitored IABs is the Manchester Road Overbridge between Denton and Middleton: two side-by-side 40m span IBs with no skew and 7m high abutments carrying the A62. The strain in, and the earth pressure acting on, the abutments were monitored during construction and throughout the first two years of service. The first bridge was a conventional portal frame structure retaining granular backfill, while the second was constructed with contiguous bored pile abutments founded on glacial till. As the bridge deck expanded, lateral stresses increased, demonstrating a strong correlation between lateral stresses and bridge temperature (Barker and Carder, 2000).

Similarly monitored was a two-span, skewed IB of 50 m total length consisting of pre-stressed concrete beams and cast in-situ deck structurally connected to full height, 9m high abutments founded in magnesian limestone over the M1-A1 Link Road at Bramham Crossroads, North Yorkshire. The field measurements (displacements of the abutment and deck; strains in the abutment and deck; earth pressures on the abutment) were recorded during construction and over the first three years of service. The measured lateral earth pressures after backfilling were consistent with predictions using the coefficient of earth pressure at rest (K_0), calculated based on the estimated friction angle (ϕ'), while they increased slightly for each of the following summers (Barker and Carder, 2001).

The results from both monitoring campaigns were invaluable, yet they only cover a relatively short period after construction whereas longer-term monitoring would be needed to determine the expected pattern of significant earth pressure escalation after more seasonal cycles; this would also have provided a better return on investment from the instruments installed (Barker and Carder, 2000; 2001).

A 15-degree skew, two-span IB of 90.9 m total length with 2.88 m high abutments in Trenton, New Jersey (USA), was monitored for a year. Abutment strains and soil pressures behind the abutment were monitored by the New Jersey Department of Transportation when revising the design specifications for integral bridges (Hassiotis et al., 2005). A steady build-up of soil pressures behind the abutment was observed.

A no-skew three-span IB of 82.3 m total length with 3.05 m high abutments spanning the Millers River between the towns of Orange and Wendell, USA, was monitored from 2002 to 2004, including longitudinal and transverse bridge displacements, backfill pressure distribution behind the abutment and abutment strains. The peak earth pressure at 2.5 m from the abutment top was observed to increase annually from 245 kPa (2002) to 280 kPa (2003) and 315 kPa (2004); similar earth pressure increases were observed at other depths behind the abutment (Brena et al., 2007).

The Van Zylspruit River Bridge (a five-span IB of 90.45 m total length with no skew and 6.6 m high abutments, located on the N1 in South Africa) exhibited a maximum earth pressure significantly (~1.75 times) higher than the at rest pressure (Skorpen et al., 2018).

Table 2. Summary information of monitored IABs

Reference	**Location**	**Span length (m)**	**Skew degree**	**Hight of abutment (m)**	**Key monitoring findings**
Barker and Carder, 2000	Manchester, UK	40	0	7	first two years of service, measured lateral stresses increased
Barker and Carder, 2001	North Yorkshire, UK	50	skewed	9	first three years of service, measured lateral earth pressures increased slightly for each of the following summers
Hassiotis et al., 2005	Trenton, New Jersey, USA	90.9	15	2.88	A steady build-up of soil pressures behind the abutment was observed
Brena et al., 2007	Millers River, USA	82.3	0	3.05	The peak earth pressure at 2.5 m from the abutment top was observed to increase annually.
Skorpen et al., 2018	Van Zylspruit River, South Africa	90.45	0	6.6	First of year of service, a maximum earth pressure significantly (~1.75 times) higher than the at rest pressure

It is clear from the published literature that there is no more than ten years of reliable monitoring data available for IBs, whereas backfill stress measurements are required for a bridge that has been in service for more than a decade (Lock, 2002). It is currently unclear whether earth pressures would continue to increase, or increase asymptotically, or level off to a steady value towards the end of the bridge's service-life (implying a hypothetical need for a 120-year observation period; Yap, 2011). Longer-term monitoring campaigns, notably focussing on the lateral soil pressure behind the abutment and incorporating redundancy to allow for instrumentation failures, are therefore essential; linking the data feeds to digital twins would further improve understanding of IB behaviour, improve designs and inform maintenance strategies.

4. Previous laboratory experimental research on IBs

4.1 Lateral earth pressure

Increases in IB backfill pressure or lateral earth pressure, which is related to the soil stiffness and strength and is dominated by the compaction of the granular backfill, have been confirmed by cyclic triaxial tests on Leighton Buzzard Sand that simulated the stress path that a typical IB abutment might impose on its retained soil (Xu, 2005). In a centrifuge model study of a spread-base integral bridge abutment assembled in a (677 × 192 × 535 mm) strongbox, the measured lateral earth pressure increased with the amplitude of the passive displacements and the number of cycles, but at a decreasing rate (Ng et al., 1998). This progressive increase in lateral stresses was also observed when the active state was reached at the end of each cycle in laboratory triaxial tests on specimens of Leighton Buzzard sand subjected to the stress paths and levels of cyclic straining that typical IB abutments might impose on its retained soil (Clayton et al., 2006). Tapper and Lehane (2005) describe a centrifuge experiment on a pinned base abutment in a (510 × 200 × 245mm) strongbox characterised by increasing displacements (d/H 0.10%, 0.40% and 1.26%), which showed that lateral stress did indeed increase until the passive limit was reached. In small-scale (1140 × 570 × 300 mm) 1g testing, the lateral stress first increased significantly (around 25 cycles), then the increase slowed (around 50 cycles), approaching asymptotically a steady-state condition (England et al., 2000). This is anticipated, as the vertical effective stresses are approximately constant, so an unbounded increase in lateral stresses is impossible, requiring an infinite magnitude of shear stress within the backfill.

Centrifuge tests in a (677 × 192 × 535 mm) strongbox by Springman et al. (1996) used embedded and spread-base abutments retaining Leighton Buzzard sand; they observed that the rate of stress increase on the back of the abutment was much reduced after the first 20 cycles. The upper limits of the stress escalation, however, are not well known (England et al., 2000). This earth pressure escalation was attributed to two distinct mechanisms: the arching effect at small amplitudes and granular flow at large amplitudes. The arching mechanism reduces the vertical stresses acting on the soil behind the lower half of the wall, resulting in lower horizontal earth pressures at this point. A dominant arching mechanism relates to small wall rotations while a dominant flow mechanism relates to large wall rotations (Tsang et al., 2002). The flow mechanism allows a continuous deformation of the soil mass in one direction. The build-up of lateral pressure was explained by the flow of granular materials during cyclic loading, known in the literature as strain ratcheting (Hassiotis et al., 2005). The significant pressure build-up was attributed to sand particle flow and densification due to cyclic loading, as well as the shearing of dense sand during bridge expansion (Khodair and Hassiotis, 2005).

There seems to be agreement based on the published evidence that the lateral pressure behind an IB abutment increases with sufficient displacement of the abutment under thermal loading. However, it remains unclear whether the lateral pressure behind the abutment will continue building up at a specific rate eventually stabilising. Furthermore, the different soil types and construction conditions make this situation more complex. Therefore, monitoring of lateral soil pressure behind abutments is needed to obtain a full understanding of IB behaviour under thermal loading. An overview of the main features of experimental studies on earth pressures in IABs is provided in Table 3.

Table 3. Dimensions of available model tests

Model	h [mm]	test type	aspect ratio				abutment material	backfill material	constraint abutment
			w/h	t/h	h/H	L/h			
England et al. 2000	570	1g pseudo-static	0.53	0.035*	1	2	metal	Leighton Buzzard	Fixed-hinged
Springman et al. 1996	110/115.9	60g centrifuge	1.88/162	0.099/0.085	0.45/0.53	2.9/2.5	dural/steel	Dry sand	Embedded/spread-base
Cosgrave and Lehane 2003	1000	1g pseudo-static	0.3	0.025	1	2.61	mild steel plate	Dry siliceous sand	hinge
Lehane 2011	160/200	(20; 25; 37.5; 40) g centrifuge	0.8/1	0.1/0.08	0.65/1	3.19/2.55	aluminium	Fine sand/ Glass ballottini/ High-OCR kaolin	hinge

h: height, w: width, t: thickness of the abutment; H: height, L: length of the backfill
*Estimation from the diagram proposed in the paper

4.2 Backfill settlement

Soil settlement has been observed when IBs are subjected to cyclic loading in centrifuge models of a spread-based abutment (Ng et al., 1998) and scale-model retaining walls (England et al., 2000), some authors even observed a gap developing between the soil behind the abutment and the wall (David and Forth, 2011). The significant settlement behind the abutment reported by Ng et al. (1998) was attributed to soil densification, strain ratcheting, horizontal sliding and the rocking motion of the abutment, while Springman et al. (1996) warned against using loose backfill behind an IB abutment to prevent excessive soil settlements. Lock (2002) noted that settlement due to thermal displacement of the IB deck is often addressed by incorporating an approach slab, whereas Hoppe (1999) suggested this to be unnecessary if the backfill is properly compacted.

The UK Design Manual for IBs (DMRB; BA42/96, 2003) does not mention the use of approach slabs, although backfill compaction is recommended to limit the soil settlement due to thermal displacement of the structure. Indeed, a survey of the UK's Highway Agency maintenance records of existing IBs revealed that, aside from isolated cases, most bridges showed no settlement problems (Yap, 2011); other field studies produced similar findings, with very few reporting soil settlement issues (Lock, 2002), emphasising the need for, and effectiveness of, good control of compaction specifications.

4.3 Effect of soil backfill

In the UK, free-draining backfill is specified in DMRB (BA42/96, 2003) as well-graded granular material with particle sizes up to 75 mm (gravel), which could include constituents such as natural gravel, natural sand, crushed gravel, crushed rock, crushed concrete, slag or chalk. It further specifies representative values of peak effective cohesion (c'_{peak}) and peak effective friction angle (φ'_{peak}) should be based on the compaction to 95% of the maximum dry density in accordance with BS1377: part 4 (BSI 1990) using the vibrating hammer method. The zone of granular backfill should extend from the bottom of the abutment wall to at least a plane inclined at 45° to the wall. According to Al-Ani et al. (2018), the backfill behind the abutment should be compacted over at least the height of abutment and vertically below the bottom of the abutment for about 25% of the abutment height.

Shah et al. (2008) state that the magnitude and mode of deformation of the backfill, the overall soil response and the overall structural response are all heavily influenced by the level of compaction in the granular fill behind the abutment, along with the relative flexural stiffness of the bridge deck, the abutment wall and any foundation piles, the lateral pressure of the soil behind the wall, and the confining stress level in the soil. This complex set of interdependencies is further complicated by lateral earth pressure build-up in granular being not solely be due to densification, but readjustment of the soil fabric due to particles reorienting under cyclic loading or straining (Fleming and Rogers, 1995), and hence compaction processes should replicate this action (i.e. using a vibrating roller rather than vertical compaction technology). Particle shape is therefore an additional consideration since it influences this readjustment in soil fabric (Yap, 2011).

The boundaries of design are being pushed further with the use of innovative backfill materials (e.g. elastic inclusions – a block of elastic material placed between the abutment wall and the retained soil) and approach slabs – such as in a US IB of 300m total length that is performing well without cracking and settlement of the pavement (Frosch, 2002). However, standard guidance on design and detailing of approach slabs (e.g. the connection to the abutment backwall, and the interface between the approach slab and approach fills) is lacking.

It is evident that a focus on backfill compaction (intensity, rotation of principal stresses, layer thickness and confinement) could lead to decrease the build-up of pressure on the IB abutment and substantially avoid backfill settlement. However, backfill compaction is not straightforward to control in IB construction processes, therefore poorly-compacted backfill should be investigated alongside well-compacted granular backfill taking cognisance of material types and gradings used in road foundations to limit permanent deformation.

5. PLEXUS pump-priming experimental campaign

To investigate the soil-structure interaction uncertainties related to the backfill behaviour behind IBs and establish the efficacy of different sensing technologies, a PLEXUS 1g small-scale soil box experimental campaign was devised, thus also paving the way for experimentation at or near full-scale in the Soil-Foundation-Structure Interaction Laboratory (SoFSI) at the University of Bristol.

The PLEXUS rig was designed to simulate the effect on the backfill from abutment displacements due to seasonal expansion and contraction of the bridge deck. The monitoring regime included lateral stresses behind the abutment wall (pressure cells), the backfill surface displacement (LVDTs) and backfill soil deformation behind the abutment (Particle Image Velocimetry, PIV). Initial tests included the backfill material being loaded by a moving abutment wall having two different relative stiffnesses (i.e., flexible and rigid abutments), the displacements replicating horizontal thermal loading conditions associated with increasing cyclic displacements and multiple-cycle constant-displacement histories.

5.1 Experimental configuration

The 1525 × 1050 × 1150 mm test box accommodated the loading system (actuator) and a 1000 × 1000 × 1000 mm specimen of backfill. A 1000 mm high moveable wall was hinged at the bottom of the soil box to simulate an IB abutment able to rotate about its base. The movable wall consisted of a 25 mm Perspex and 25 mm timber composite to simulate a flexible abutment wall, while the rigid movable wall consisted of a 25 mm Perspex, 25 mm timber composite, 50 mm aluminium frame and 25 mm timber composite producing a sandwich configuration. Perspex was used for the box wall to enable PIV observations of backfill displacements, while the remainder of the rig was designed without metal components to facilitate future trialling of a ground penetration radar as a monitoring tool (see Figure 5). The abutment wall, end wall and side wall were instrumented with pressure cells, while LVDTs were used to measure surface backfill displacements. The backfill consisted of uniform Leighton Buzzard sand fraction B (see Fiorentino et al. 2021).

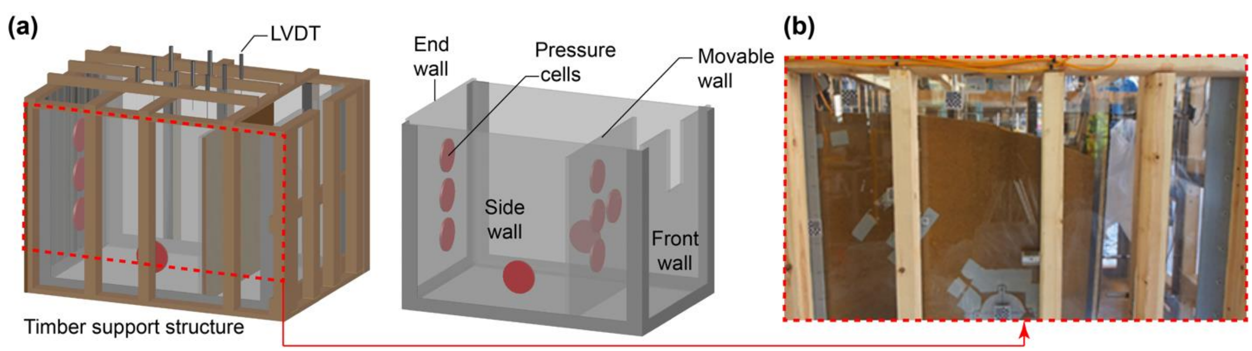

Figure 5. (a) an annotated 3D diagram of the test box, (b) the test box filled with Leighton Buzzard (LB) sand.

5.2 Thermal loading

Thermal loading from temperature-induced cyclic expansion and contraction of the bridge deck was simulated by push-pull pseudo-static motion of the moveable wall, its displacement being controlled by the actuator mounted 870 mm above the wall base. In Test#1, the flexible abutment wall was subjected to 12 loading cycles with a loading rate of 0.5 mm/s (to simulate static thermal loading, Springman et al., 1996; Lehane, 2011), each cycle lasting at least 40 seconds. The cyclic displacements at the top of the movable wall started at ±5 mm, with increments of ±5 mm every two cycles, to reach ± 30 mm (drift ~3.5×10^{-2}; see Table 4). In Test#2, the rigid abutment wall was subjected to 59 'loading' cycles with a loading rate of 1.0 mm/s and cyclic displacements at the top of wall fixed at ±30 mm for each cycle (1 mm/s was considered slow enough to simulate static thermal loading). The 30mm equals the seasonal deck movement (one end) of a IAB in London with a 131m length concrete deck or a 91m length of steel deck (England et al. 2000).

5.3 Instrumentation layout

The instrumentation employed consisted of TPC-4000 series Total Earth Pressure Cells (TEPCs) to measure lateral stresses, and Linear Voltage Differential Transducers (LVDTs) and a high-resolution camera on the side of the test-rig to measure displacements. The TEPCs are designed to measure total pressure (combined effective stress and pore water pressure) in soils and at soil-structure interfaces yet, as the Leighton Buzzard Sand was dry, they directly provided effective stress measurements. The locations of the three end wall TEPCs (1-3), four moveable wall TEPCs (6-9) and sidewall TEPCs (4 and 5) are shown in Figure 6.

Table 4. Summary information for Tests #1 and #2.

Test ID	Abutment Wall	Total Cycles	Loading Rate [mm/s]	Displacement history [mm] & Drifts
#1	Flexible Perspex +Timber[1]	12	0.5	$2 \cdot \{\pm 5mm; \pm 10mm; \pm 15mm; \pm 20mm; \pm 25mm; \pm 30mm\}$ $2 \cdot \{(\pm 5.7; \pm 11.5; \pm 17.2; \pm 23.0; \pm 28.7; \pm 34.5) \times 10^{-3}\}$
#2	Stiff Sandwich section[2]	59	1.0	$59 \cdot \{\pm 30\ mm\}$ $59 \cdot \{\pm 34.5 \times 10^{-3}\}$

[1] 25 mm Perspex + 25 mm Timber
[2] 25 mm Perspex + 25 mm Timber + 50 mm Aluminium frame + 25 mm Timber

Figure 7 shows the positions of the nine LVDTs (1-9) placed in three rows on the backfill surface and four LVDTs (11-13) measuring the moveable (abutment) wall displacement. The high-resolution camera (Canon 70D 5472*3648 pixels) focussed on the Perspex sidewall to record ‘full-field’ backfill deformation using the PIV method, regarded as slow “fluid motion” (Stanier et al., 2010).

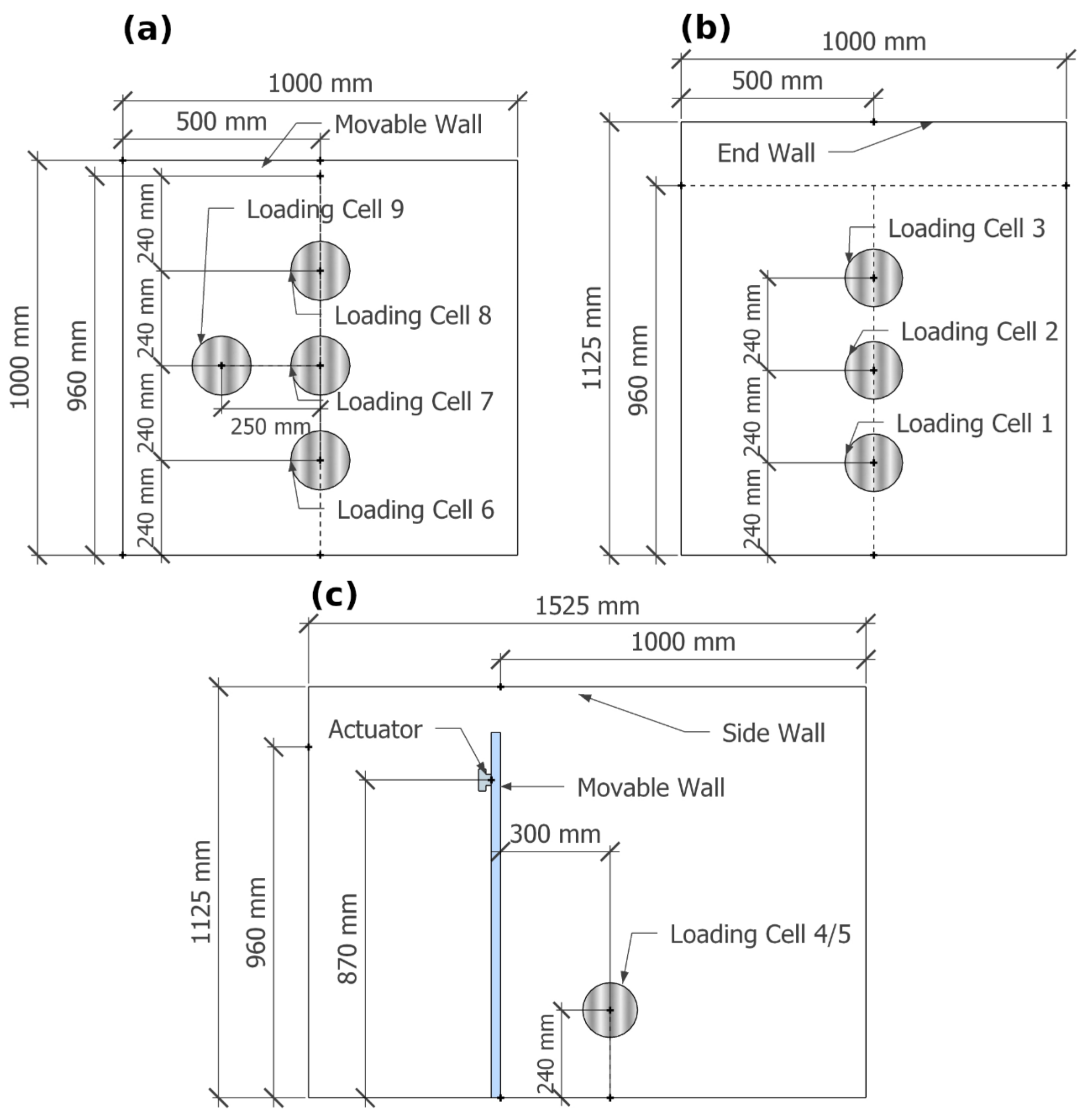

Figure 6. The layout of the pressure cells in the test box: (a) movable wall, (b) end wall, (c) sidewall including exact position of actuator.

5.4 Backfill

The backfill material selected was Leighton Buzzard Sand (LBS) fraction B (Lings and Dietz, 2004; Kloukinas et al., 2015; Fiorentino et al., 2021), having dry densities in Test #1 and Test #2 of 1.48 Mg/m^3

and 1.44 Mg/m^3, respectively. The minimum and maximum dry densities for the LBS were determined as 1.48 Mg/m^3 and 1.65 Mg/m^3. The density value in Test #2 obtained is slightly lower than the minimum provided by Fiorentino et al. (2021) but this is likely due to the absence of compaction and no control of density at the different filling stage leading to an overall figure that is about right within the tolerance of the process implemented experimentally. The specific gravity of LBS grains was 2.65, while the minimum and maximum void ratios (e_{min} and e_{max}), were 0.35 and 0.83, respectively (Fiorentino et al., 2021). To achieve a uniform, relatively loose LBS specimen, the sand was pluviated into the soil box in three layers, with levelling (but no compaction) applied after each pour.

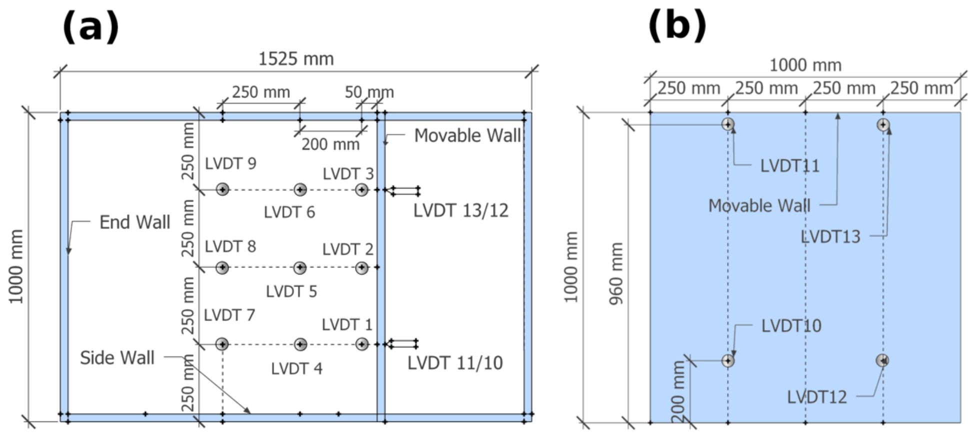

Figure 7. The layout of the LVDTs (a) plan view of the test box, (b) front view of the movable wall.

5.5 Results

The two tests have multiple differences (i.e., wall stiffness, 'loading' rate, displacement history increasing or kept constant), making a systematic comparison difficult. Nevertheless, in Figure 8a, a preliminary comparison is proposed between the earth pressure distributions obtained using Rankine theory and PD6694 (see Figure 4 and Equation 4) and the passive-like pressure recorded at three instants: (a) at cycle 12 of Test #1 (i.e. the second cycle at +30 mm after the increasing displacement history), (b) at cycle 2 of Test #2 (i.e. the second cycle at +30 mm), and (c) at cycle 12 of Test #2 (i.e. the twelfth cycle at +30 mm). The vertical distance from ground level to the assumed point of rotation of the abutment (H) is 0.96 m, while the wall deflection at depth $H/2$ below ground level (d_d') was 0.7 times the horizontal movement of the end of the bridge deck. C is 20 assuming that the Young's modulus of the sand is less than 100 MPa. The critical friction angle was taken as $\phi_{cs} = 32°$ and the elastic modulus as 20 MPa (Ng et al., 1998). The coefficient of passive earth pressure ($K_{p;t}$) was obtained through linear interpolation for values of ϕ_{cs} between 30° ($K_{p;t} = 4.29$) and 35° ($K_{p;t} = 5.88$) for a non-smooth vertical wall with δ/ϕ' = 0.5 retaining a horizontal backfill (see Table 8 in PD6694 2011).

The lateral soil pressures measured in both tests were larger than the pressures calculated according to Equation 4 from PD6694 (see Section 2) using the maximum and minimum LBS densities. This may be caused by the specific configuration of the experiments and the influence of the backwall (as the distance between the abutment and the backwall was 1 m when at least 1.7 m would be necessary to develop a complete passive failure wedge). However, the shape of the lateral pressure distribution on the abutments, resulting from the three experimental measurement points, mimics the shape of the envelope proposed by PD6694. The lateral pressure on the abutment after the 12th cycle in Test #2 was larger than that after the 12th cycle in Test #1, attributed to the larger cyclic lateral displacement in Test #2 (an expected result) and/or the lower stiffness of the abutment wall in Test#1 (also an expected phenomenon).

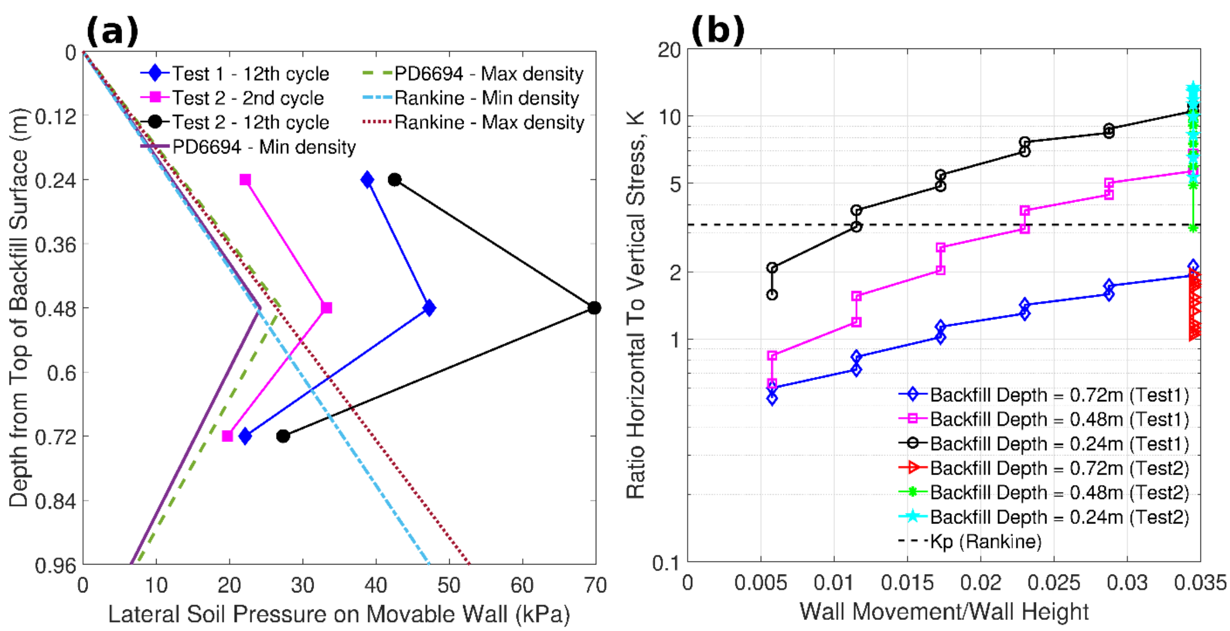

Figure 8. (a) Measured earth pressures and (b) ratio of horizontal to vertical stress when wall is moving into the backfill soil (passive).

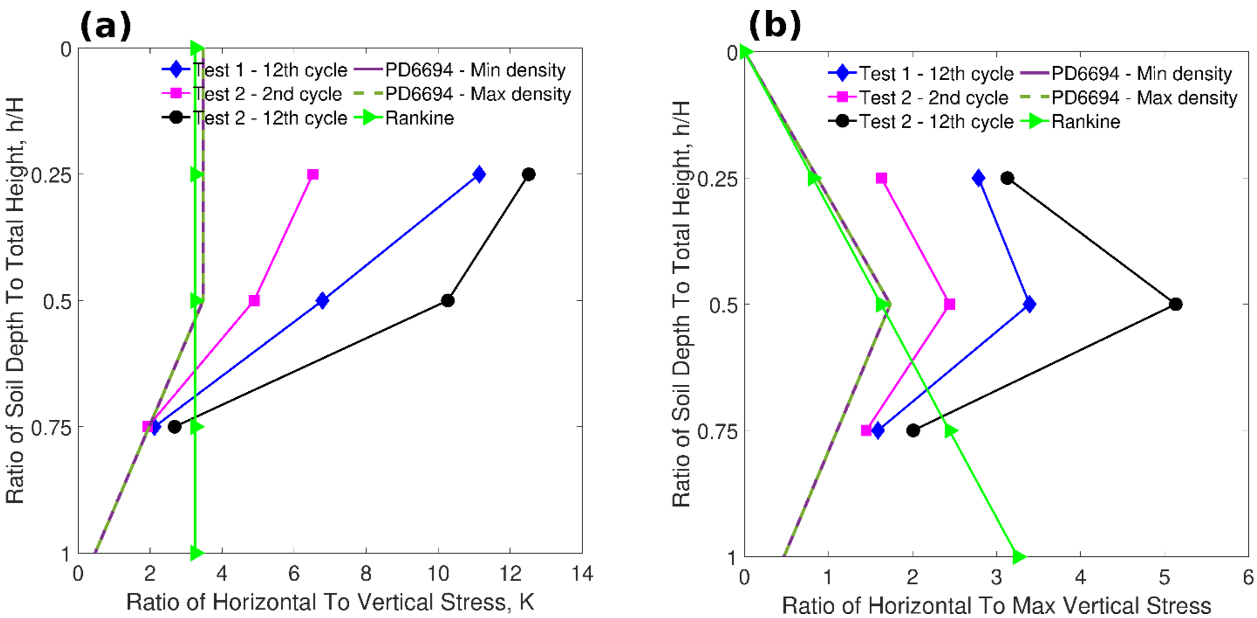

Figure 9. Normalised distributions of earth pressures with depth: (a) x axis normalised by γz and (b) x axis normalised by γH represented against y axis normalised by total height of the soil (H = 96 cm).

The lateral soil pressures on the movable wall in Figure 8a were normalised separately by the vertical stress, γz, *where* γ is united weight, z is the soil depth (Figure 9a), and by the maximum vertical stress, γH, where H is the total depth of the soil (Figure 9b), thereby making them scalable for general translation. The vertical axes of Figure 9 are normalised by the total height of the backfill. The ratios of horizontal to vertical stress measured by the bottom pressure cell at cycle 12 in Test #1 and at cycle 2 in Test#2 were very close to that calculated from PD6694, while the pressure at cycle 12 in Test #2 is larger.

In Test #2, the lateral pressure on the stiffer abutment after 12 cycles was larger than after 2 cycles (all cycles consisting of ±30 mm displacement). Figure 8b shows the rapid increase in lateral soil pressure with increasing number of cycles and displacements (up to cycle 12) in Test #1, and with constant displacement and increasing cycles in Test #2, compared with the theoretical passive Rankine value and comparative values suggested by NCHRP (1991) and NAVFAC (1982) shown in Figure 3a.

Backfill surface settlement is significantly smaller for the stiffer abutment after 2 cycles than after 12 cycles (Figure 10). The settlements rapidly increased with the number of cycles. The settlement behind the stiff abutment after 12 cycles is slightly larger than for the 12th cycle behind the flexible abutment, attributed to abutment stiffness and/or amplitude of cyclic loading.

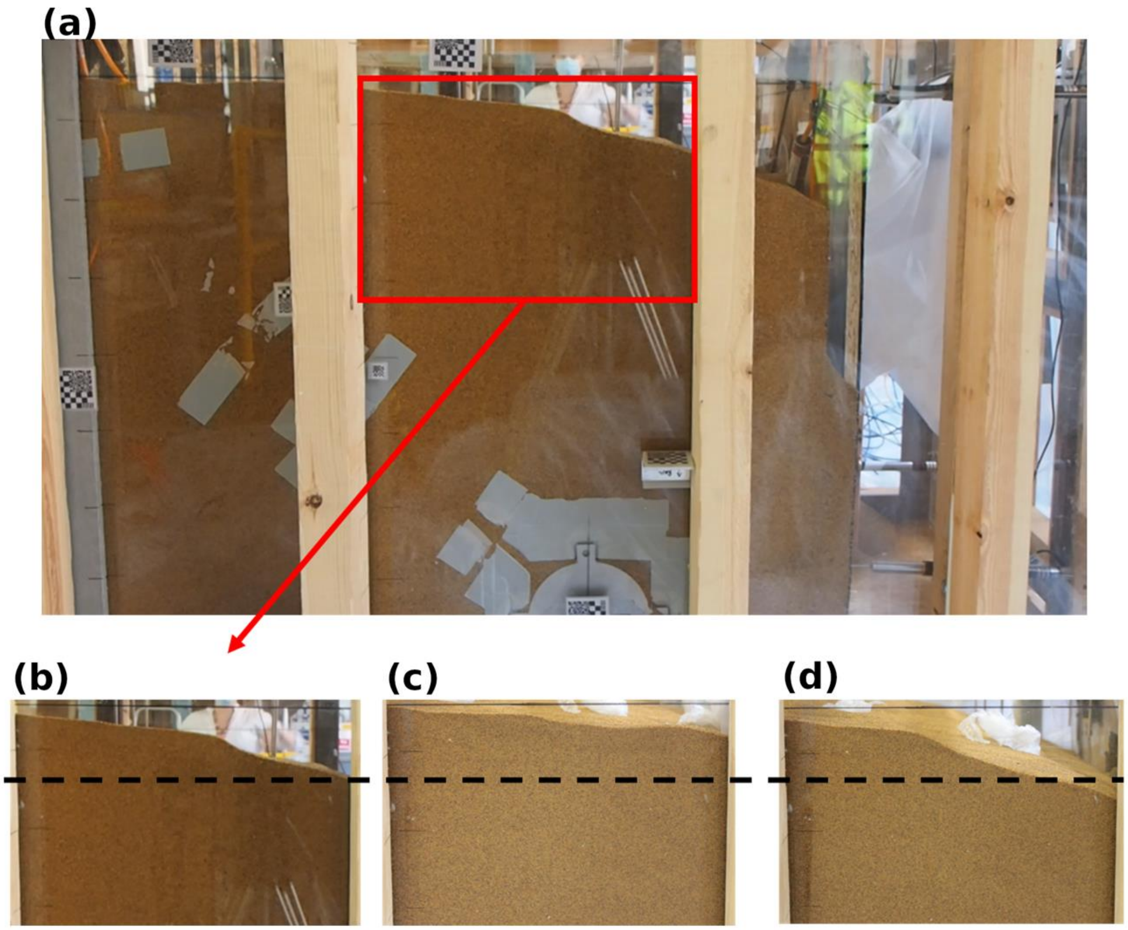

Figure 10. The settlement behaviour of the backfill, (a) Test #1 – 12th cycle, (b) Test #1 – 12th cycle (zoomed-in), (c) Test #2 – 2nd cycle (zoomed-in), (d) Test #2 – 12th cycle (zoomed-in), the black dotted line offers the same reference level for a better comparison.

The densification of the backfill in the zoomed-in areas of Figures 10b to 10d was analysed using the GeoRG PIV MATLAB analysis package (Stainer et al. 2015). As shown in Figure 11 (where volumetric strain value shown with the colour of contour and the black arrows only present the deformation direction of the soil backfill), the deformation of the backfill after 12 cycles in Test #1 (Figure 11a and 11b) was larger than that in Test #2 when the actuator was at maximum extension. In contrast, the opposite behaviour was observed when the actuator was at its maximum contraction. The lower lateral soil pressure on the flexible abutment than that on the stiff abutment was attributed to the backfill becoming denser in the stiff abutment test. The densification of the backfill after two cycles in the stiff abutment configuration (Figure 11c and 11d) is much larger than after 12 cycles (Figure 11e and 11f), thus indicating that the amplitude of the backfill densification decreases with increasing loading cycles in the same test.

It is evident from these results that abutment stiffness, number of cycles, backfill material state and the magnitude of abutment horizontal displacement are key parameters in determining IB performance, and warrant further investigation in controlled experiments. Pressure cells and PIV measurements are particularly suitable to compare the performance of different test configurations.

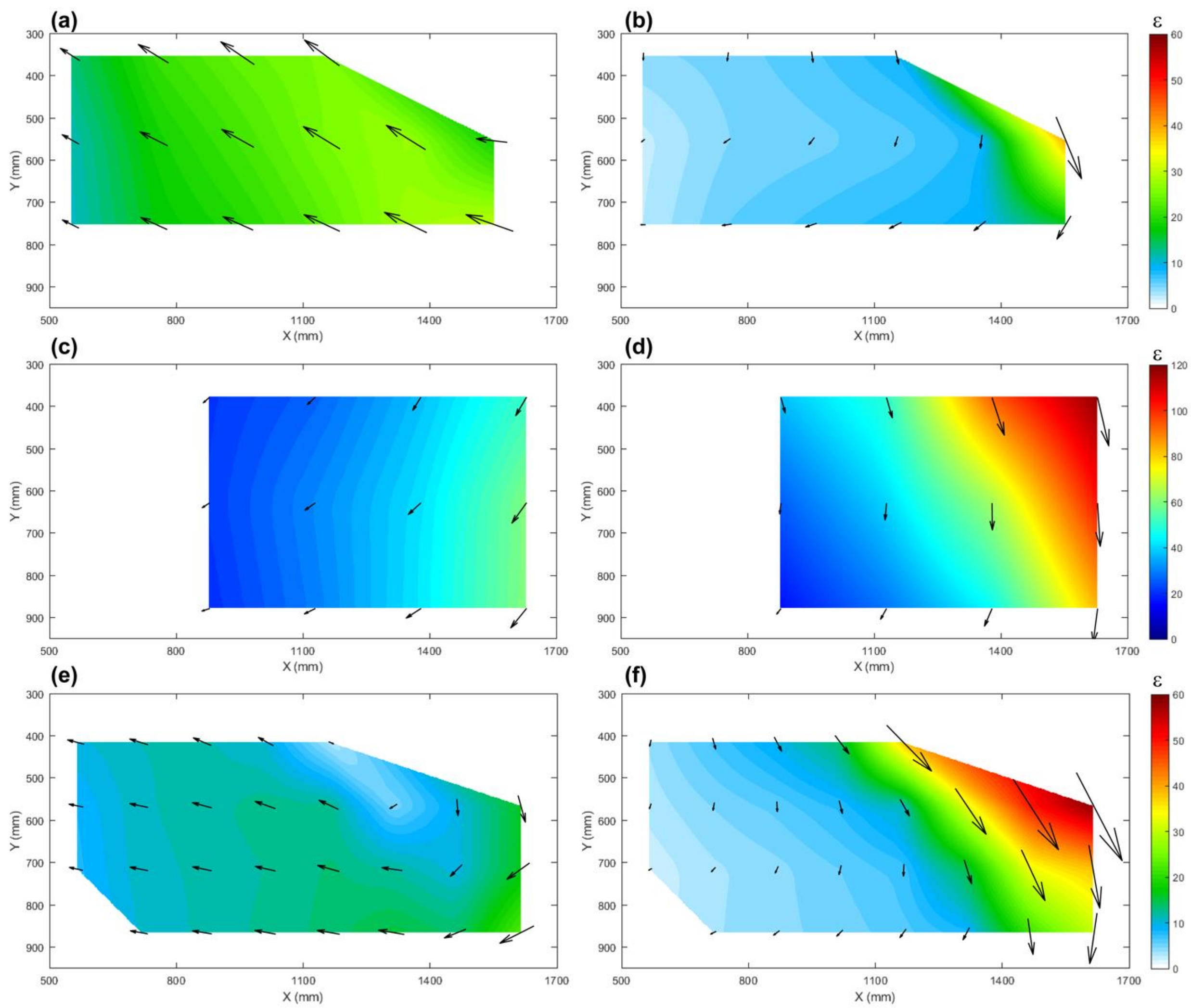

Figure 11. Percentage volumetric strain (ε) and deformation direction (black arrows) of the soil backfill: Test #1 – 12th cycle (a) maximum extension position and (b) maximum contraction position; Test #2 – 2nd

cycle (c) maximum extension position and (d) maximum contraction position; Test #2 – 12th cycle (e) maximum extension position and (f) maximum contraction position.

6. Conclusions

This paper discussed the behaviour of integral bridges (IB's) under thermal loading by reviewing: (1) current international design practices, and (2) lessons learnt from field monitoring cases and previous experimental research. The soil pressure behind the abutment wall is a crucial factor for the design and performance of integral bridges, while the backfill behind the abutments significantly influences performance. The PLEXUS experimental campaign, described herein, demonstrated the efficacy of its monitoring processes in establishing soil-structure interaction behaviour of integral bridge abutments under thermal loading and identified key research needs. In particular, pressure cells and PIV provided useful data for performance comparisons in laboratory environments, while settlements measurements proved less informative. The research revealed a need for precise density monitoring of the backfill throughout the duration of the tests and throughout the soil specimen. In the non-metallic PLEXUS test rig, this could be achieved by ground penetration radar, x-ray tomography and/or similar techniques.

The small-scale tests have created results that are suitable for analytical and numerical validation, although scaling effectiveness needs to be proven. Further, larger-scale physical model tests of integral bridge abutments, using different types of backfill compacted to counter unwanted deformations due to ratcheting (e.g. incorporating rotation of principal stresses) and to cover the variety of materials likely in practice, are required to ensure improved sustainable and resilient designs of integral bridges.

Data availability statement

All data from the Plexus experimental campaign are available from the corresponding author by request

Acknowledgements

UKCRIC PLEXUS – Priming Laboratory EXperiments on infrastructure and Urban Systems was funded by the Engineering and Physical Sciences Research Council under grant number EP/R013535/1.

UK Collaboratorium for Research on Infrastructure and Cities (UKCRIC), grant number EP/R017727/1.

References

AASHTO (2012). AASHTO LRFD Bridge Design Specifications. American Association of State Highway and Transportation Officials, Washington, DC.

AbdelSalam, S.S. and Azzam, S.A. (2016). Reduction of lateral pressures on retaining walls using geofoam inclusion. Geosynthetics International, 23(6): 395-407.

Al-Ani, M., Murashev, A., Palermo, A. et al. (2018). Criteria and guidance for the design of integral bridges. Proceedings of the Institution of Civil Engineers – Bridge Engineering, 171(3): 143–154.

BA42/96 (2003). The Design of Integral Bridges; BA 42/96, Amendment No. 1. Design Manual for Roads and Bridges (DMRB). UK: Department for Transport.

Bal, A.R.L., Hoppe, U., Dang, T.S., Hackl, K. and Meschke, G. (2018). Hypoplastic particle finite element model for cutting tool-soil interaction simulations: Numerical analysis and experimental validation. Underground Space, 3(1): 61-71.

Baptiste, K.T., Kim, W., Laman, J.A. (2011). Parametric study and length limitations for prestressed concrete girder integral abutment bridges. Structural Engineering International, 21(2):151-156.

Barker, K.J. and Carder, D.R. (2000). Performance of the two integral bridges forming the A62 Manchester road overbridge. TRL Report 436. Transport Research Laboratory, Crowthorne, Berkshire, UK.

Barker, K.J. and Carder, D.R. (2001). Performance of an integral bridge over the M1- A1 Link Road at Bramham Crossroads. TRL Report 521. Transport Research Laboratory, Crowthorne, Berkshire, UK.

Bonczar, C., BreÒa, S.F., Civjan, S.A., DeJong, J., Crellin, B., and Crovo, D. (2005). Field Data and FEM Modeling of the Orange-Wendell Bridge. Proceedings: 2005 FHWA Conference: Integral Abutment and Jointless Bridges (IAJB 2005), Baltimore, MD, 17-19 March, pp163-173.

Bloodworth, A.G., Xu, M., Banks, J.R. and Clayton, C.R.I. (2011). Predicting the earth pressure on integral bridge abutments. Journal of Bridge Engineering, 17(2): 371-381.

BMVBS (2013). Integrale Bauwerke. Bundesministerium für Verkehr, Bau und Stadtentwicklung, RE-ING (Richtlinien für den Entwurf und die Ausbildung von Ingenieurbauten), Teil 2, Brücken, Abschnitt 5. Berlin, Germany.

British Standards Institution, BS EN 1991-1-5: 2003: Eurocode 1: Actions on structures: General actions - Thermal actions. London, 2003.

British Standards Institution, BS 1377-4:1990, Methods of test for soils for civil engineering purposes. Compaction-related tests**,** *Status :* Project Underway, Current

Breña S. F., Bonczar C. H., Civjan S. A., DeJong J. T. and Crovo D. S., (2007), Evaluation of Seasonal and Yearly Behavior of an Integral Abutment Bridge, Journal of Bridge Engineering, Vol. 12, No. 3, ISSN1084-0702/2007/3-296–305

Burke Jr MP. Integral and semi-integral bridges. John Wiley & Sons 2009

Canadian Geotechnical Society., 1978. Canadian Foundation Engineering Manual, Montreal, Quebec.

Capilleri, P., Motta, E., Todaro, M. and Biondi, G., 2019, July. Experimental Study on a Three-Dimensional Passive Earth Pressure Coefficient in Cohesionless Soil. In National Conference of the Researchers of Geotechnical Engineering (pp. 545- 554). Springer, Cham.

Caristo A, Barnes J, Mitoulis SA. Numerical modelling of integral abutment bridges under seasonal thermal cycles. Proc. Inst. Civil Eng. – Bridge Engineering 2018; 171(3): 179-190

Clayton, C.R.I., Xu, M. and Bloodworth, A., 2006. A laboratory study of the development of earth pressure behind integral bridge abutments. Géotechnique, 56(8), pp.561-571.

Clough, G.W. and Duncan, J.M., 1991. Earth pressures. In Foundation engineering handbook (pp. 223-235). Springer, Boston, MA.

Cole, R.T. and Rollins, K.M., 2006. Passive earth pressure smobilisation during cyclic loading. Journal of Geotechnical and Geoenvironmental Engineering, 132(9), pp.1154-1164.

Coulomb, C. A. (1773). “Essai sur une application des règles de maximis & minimis à quelques problèmes de statique, relatifs à l'architecture.” Mémoires de mathématique & de physique présentés à l'Académie Royale des Sciences par divers savans & lûs dans ses assemblées, 7, 343–382, Paris (printed in 1776).

Cui, L. and Mitoulis, S., 2015. DEM analysis of green rubberised backfills towards future smart integral abutment bridges (IABs). Geomechanics from Micro to Macro. I, II, pp.583-588.

David, T.K., Forth, J.P., 2011. Modelling of soil structure interaction of integral abutment bridges. International Journal of Civil and Environment Engineering 5(6), 645-650.

Dhar, S. and Dasgupta, K. Seismic Soil Structure Interaction for Integral Abutment Bridges: a Review. Transp. Inf. Geotech. 2019, 6(4): 249-267.

Dicleli M, Eng P, Albhaisi SM. Maximum length of integral bridges supported on steel H-piles driven in sand. Engineering structures 2003, 25(12), 1491-1504.

Dicleli, M. 2005. Integral Abutment-Backfill Behaviour on Sand Soil-Pushover Analysis Approach. JOURNAL OF BRIDGE ENGINEERING, 10, 354-364.

EN 1997-1, Eurocode 7: Geotechnical design – Part 1: General rules. Part 2: Ground investigation and testing

England, G. L., Tsang, N. C. M. & Bush, D. I. 2000. Integral Bridges; A fundamantal approach to the time-temperature loading problem, London, Thomas Telford.

FARAJI, S., TING, J. M., CROVO, D. S. & ERNST, H. 2001. Nonlinear Analysis of Integral Bridges: Finite-Element model. Journal of Geotechnical and Geoenvironmental Engineering, Vol. 127.

Fenneman, J.L., Laman, J.A. and Linzell, D.G., 2005. Predicted and measured response of an integral abutment bridge. Journal of Bridge Engineering, 10(6), pp.666-677.

Fiorentino G, Cengiz C, De Luca F, Mylonakis G, Karamitros D, Dietz, M, Dihoru L, Lavorato D, Briseghella B, Isakovic T, Vrettos C, Topa Gomes A, Sextos A, Nuti C. Integral abutment bridges: Investigation of seismic soil-structure interaction effects by shaking table testing, Earthquake Engng Struct Dyn, (accepted). 2020:1-22, DOI: 10.1002/eqe.3409

Firoozi, A.A., Firoozi, A.A. and Baghini, M.S., 2016. A Review of Clayey Soils. Asian Journal of Applied Sciences (ISSN: 2321– 0893), 4(06).

Fleming, P.R. and Rogers, C.D.F. (1995). Assessment of Pavement Foundations During Construction. Proceedings of the Institution of Civil Engineers – Transport, 111 (2), 105-115.

Frosch, R., 2002. Modeling and control of side face beam cracking. ACI Structural Journal, 99(3): 376–385.

Gaba A., Hardy S., Doughty L., Powrie W. and Selemetas D. (2017). Guidance on embedded retaining wall design. CIRIA.

Global Infrastructural Hub, Reference Note – InfraTech Stocktake, July 2020

Gorini, D.N. and Callisto, L., 2017, June. Study of the dynamic soil-abutment-superstructure interaction for a bridge abutment. In 1st European conference on OpenSees. OpenSees days Europe (pp. 57-60).

Gorini, D.N. and Callisto, L., 2019, July. A Coupled Study of Soil-Abutment-Superstructure Interaction. In National Conference of the Researchers of Geotechnical Engineering (pp. 565-574). Springer, Cham.

Greimann, L.F., Yang, P.S. and Wolde-Tinsae, A.M., 1986. Nonlinear analysis of integral abutment bridges. Journal of Structural Engineering, 112(10), pp.2263-2280.

Griffiths, D.V. and Fenton, G.A., 2008. Risk assessment in geotechnical engineering (pp. 381-399). Hoboken, New Jersey: John Wiley & Sons, Inc

Hanna, A. and Diab, R., 2016. Passive earth pressure of normally and overconsolidated cohesionless soil in terms of critical-state soil mechanics parameters. International Journal of Geomechanics, 17(1), p.04016028.

Hassiotis, S., Lopez, J., and Bermudez, R. (2005).Full-scale testing of an integral abutment bridge. Federal Highway Association Conf. on Integral Abutment and Jointless Bridges, West Virginia Univ., Morgantown, WV.

Hoppe, E.J. (1999). Guidelines for the use, design, and construction of bridge approach slabs. Virginia Transportation Research Council, Charlottesville, Va. VTRC 00-R4

Hoppe, E.J. 2005. Field Study of Integral Backwall with Elastic Inclusion. Virginia Transportation Research Council, Charlottesville, pp. 36

Horvath JS. Integral-abutment bridges: geotechnical problems and solutions using geosynthetics and ground improvement. In West Virginia University, 2005

Horvath JS. Integral-abutment bridges: problems and innovative solutions using EPS geofoam and other geosynthetics. Res. Rpt. No. CE/GE-00, 2, 2000

Horvath, J.S., 2004. Integral-abutment bridges: a complex soil-structure interaction challenge. In Geotechnical Engineering for Transportation Projects (pp. 460-469).

Huffman, J.T., Xiao, F., Chen, G. and Hulsey, J.L., 2015. Detection of soil-abutment interaction by monitoring bridge response using vehicle excitation. Journal of Civil Structural Health Monitoring, 5(4), pp.389-395.

Kappos AJ, Sextos, AG. Seismic assessment of bridges accounting for nonlinear material and soil response, and varying boundary conditions. In Coupled site and soil-structure interaction effects with application to seismic risk mitigation (pp. 195-208). Springer, Dordrecht, 2009.

Karpurapu R, Bathurst RJ. Numerical Investigation of Controlled Yielding of Soil-Retaining Wall Structures. Geotext Geomembranes 1992; 11(2):115-131

Keykhosropour, L. and Lemnitzer, A., 2019. Experimental studies of seismic soil pressures on vertical flexible, underground structures and analytical comparisons. Soil Dynamics and Earthquake Engineering, 118, pp.166-178.

Khodair, Y. A. & Hassiotis, S. 2005. Analysis of Soil-Pile Interaction in Integral Abutment. Computer and Geotechnics, 32, 201-209.

Kloukinas P, Scotto di Santolo A, Penna A, Dietz M, Evangelista A, Simonelli AL, Taylor C, Mylonakis G. Investigation of seismic response of cantilever retaining walls: Limit analysis vs shaking table testing. Soil Dyn Earthq Eng 2015; 77:432-445.

Kotsoglou AN, Pantazopoulou SJ. Assessment and modeling of embankment participation in the seismic response of integral abutment bridges. Bull Earth Eng. 2009; 7(2):343.

Kotsoglou, A, Pantazopoulou S. Bridge–embankment interaction under transverse ground excitation. Earthquake Engineering & Structural Dynamics 2007, 36(12): 1719-1740.

Lings ML, Dietz MS. An improved direct shear apparatus for sand. Géotechnique 2004. 54(4):245-256.

Lock, R.J. *Integral Bridge Abutments*. Master of Engineering Project Report. University of Cambridge, Department of Engineering, Cambridge, U.K., 2002.

Mahjoubi, S. and Maleki, S., 2018. Finite element modelling and seismic behaviour of integral abutment bridges considering soil–structure interaction. European Journal of Environmental and Civil Engineering, pp.1-20.

Massachusetts Bridge Manual, Part I, December 1999

McCallen DB, Romstad KM. Dynamic analyses of a skewed short-span box-girder overpass. Earthq Spectra. 1994; 10(4):729-756.

Mei, G.X., Chen, R. and Liu, J., 2017. New insight into developing mathematical models for predicting deformation dependent lateral earth pressure. International Journal of Geomechanics, 17(8), p.06017003.

Muttoni, A., Dumont, A.-G., Burdet, O., Savvilotidou, M., Einpaul, J., Nguyen, M. L., Experimental verification of integral bridge abutments, Rapport OFROU, Switzerland, 2013.

Mitoulis SA, Palaiochorinou A, Georgiadis I, Argyroudis S, Extending the application of integral frame abutment bridges in earthquake-prone areas by using novel isolators of recycled materials. Earthq Eng Struct Dyn. 2016,45(14):2283-2301.

Mylonakis G, Papantonopoulos KI, Chrysikos DA. (2007a) New Analytical solutions for Retaining Structures under Static and Dynamic Loads. XIV European Conference on Soil Mechanics and Geotechnical Engineering 2007b, 24-27 September, Madrid, Spain. 6 pages on CD-ROM 3:1497-1503

Mylonakis G, Kloukinas P, Papantonopoulos K. (2007b). An Alternative to the Mononobe-Okabe Equations for Seismic Earth Pressures, Soil Dynamics & Earthquake Engineering, 27(10): 957-969.

National Infrastructure Delivery Plan (2016-2021). HM Treasury and Cabinet Office, London, UK. ISBN 978-1-910835-77-7

NAVFAC (1982). Foundations and Earth Structures Design Manual 7.2. Department of the Navy, Alexandria, Virginia, USA.

NCHRP (1991). Manuals for design of bridge foundation. Report 343. Transportation Research Board, Washington DC, USA. ISSN: 0077-5614

Ng, C.W.W., Springman, S.M. & Norrish, A.R.M. (1998). Centrifuge modeling of spread-base integral bridge abutments. Journal of Geotechnical and Geoenvironmental Engineering, 124, 376-388

National Institute of Standards and Technology NIST (2015). Community resilience planning guide for buildings and infrastructure systems, volumes I and II. Available at: http://dx.doi.org/10.6028/NIST.SP.1190v1

Nuti C, Rasulo A, Vanzi I. Seismic assessment of utility systems: Application to water, electric power and transportation networks. In Safety, Reliability and Risk Analysis: Theory, Methods and Applications, Proceedings of the Joint ESREL and SRA-Europe Conference 2009, Valencia, Spain (pp. 22-25).

Pain, A., Choudhury, D. and Bhattacharyya, S.K., 2017. Seismic passive earth resistance using modified pseudo-dynamic method. Earthquake Engineering and Engineering Vibration, 16(2), pp.263-274.

Paraschos A, Amde AM. A survey on the status of use, problems, and costs associated with Integral Abutment 871 Bridges. Better Roads. 2011; 1-20.

Paraschos, A. (2016). *Effects of wingwall configurations of the behaviour of integral abutment bridges.* PHD Thesis. University of Maryland, US.

PD 6694-1: 2011. Recommendations for the Design of Structures subject to Traffic Loading to BS EN 1997-1. BSi, London

Rajesh, BGG and Choudhury, D., 2017. Seismic passive earth resistance in submerged soils using modified pseudo-dynamic method with curved rupture surface. Marine Georesources & Geotechnology, 35(7), pp.930-938.

Rasulo A, Goretti A, Nuti C. Performance of lifelines during the 2002 Molise, Italy, earthquake. Earthq Spectra 2004; 20(S1): S301-S314.

Shah BR, Peric D and Esmaeily A(2008) Effects of Ambient Temperature Changes on Integral Bridges. Kansas Department of Transportation, Topeka, KS, USA, Technical report K-TRAN: KSU-06-2

Shamsabadi, A., Rollins, K.M. and Kapuskar, M., 2007. Nonlinear soil–abutment–bridge structure interaction for seismic performance-based design. Journal of geotechnical and geoenvironmental engineering, 133(6), pp.707-720.

Skorpen, S. A., Kearsley, E. P. & Kruger, E. J. (2018) Measured temperature and shrinkage effects on a 90 m long integral bridge in South Africa. Proceedings of the Institution of Civil Engineers - Bridge Engineering 171(3):169-178, https://doi.org/10.1680/jbren.17.00019.

Springman, S. M., Norrish, A. R. M. & NG, C. W. W. 1996. Cyclic Loading of Sand Behind Integral Bridge Abutments. TRL Report; 146. Crowthorne: Transport Research Laboratory.

Stanier, S.A., Blaber, J., Take, W.A. and White, D.J. (2015). Improved image-based deformation measurement for geotechnical applications. Canadian Geotechnical Journal, doi: 10.1139/cgj-2015-0253.

Tapper, L & Lehane, B 2005, Lateral stress development on integral bridge abutments. in AJ Deeks & H Hao (eds), *Developments in Mechanics and Structures of Materials.* Perth, Australia edn, vol. 2, CRC

Press/Balkema, The Netherlands, pp. 1069-1075, Lateral stress development on integral bridge abutments, 1/01/05.

Thoft-Christensen P. Infrastructures and life-cycle cost-benefit analysis. Struct Infrastruct E. 2012; 8(5). 507-516

Tsang, N. C. M., England, G. L. & Dunstan, T. 2002. Soil/Structure Interaction of Integral Bridge with Full Height Abutments. 15th ASCE Engineering Mechanics Conference June 2-5, 2002, Columbia University. New York.

Vahedifard, F., Leshchinsky, B.A., Mortezaei, K. and Lu, N., 2015. Active earth pressures for unsaturated retaining structures. Journal of Geotechnical and Geoenvironmental Engineering, 141(11), p.04015048.

White H, Pétursson H, Collin P. Integral abutment bridges: the European way. Practice periodical on structural design and 895 construction 2010; 15(3):201-208.

Wolde-Tinsae, A.M. and Greimann, L.F., 1988. General design details for integral abutment bridges. Civil Engineering Practice, 3(2), pp.7-20.

Xu, S.Y., Kannangara, K.P.M. and Taciroglu, E., 2018. Analysis of the stress distribution across a retaining wall backfill. Computers and Geotechnics, 103, pp.13-25.

Yap, F. L. (2011) The application of the discrete element method to integral bridge backfill. *University of Southampton, Faculty of Engineering and the Environment, Doctoral Thesis*, 194pp.

Yazdandoust, M., Panah, AKK and Ghalandarzadeh, A., 2019. Effect of reinforcing technique on strain-dependent dynamic properties of reinforced earth walls. Soils and Foundations.

Zhang and Makris 2002, Kotsoglou and Pantazopoulou 2007, 2009; Kappos and Sextos 2009, + the reference appeared in later part)

Zhang J, Makris N. Seismic response analysis of highway overcrossings including soil–structure interaction. Earthq Eng Struct Dyn. 2002; 31(11):1967-1991.

Zordan T, Briseghella B, Lan C, Analytical formulation for limit length of integral abutment bridges. Struct Eng Int 2011b, 21(3): 304-310.

Zordan T, Briseghella B, Lan C. Parametric and pushover analyses on integral abutment bridge. Eng Struct 2011a; 33(2):502-515.